Int. Journ. of Wettability Science and Technology, Vol. 1, pp. 137–167
Reprints available directly from the publisher.
Photocopying permitted by license only.

The Quality Assessment of a Mudtherapy Protocol by Surface Tensiometry Using the Contact Angle Method: The Japanese Biofango® Therapy Experience

R. DAVIDE[1,2,*]

[1]*Department of Pharmaceutical and Pharmacological Sciences, University of Padova, Via Marzolo 5-35131 Padova, Italy*
[2]*Faculty of Bioscience and Technology for Food Agriculture and Environment, University of Teramo, Via R. Balzarini, 1-64100 Campus Coste Sant'Agostino, Teramo, Italy*

The hydration state of human skin depends on good functionality of the epidermal selective barrier which is dictated by the stratum corneum. The link between the hydration state of skin and the functional effects of formulations and natural systems, such as thermal muds, has been demonstrated by several studies. Thermal muds have hydration properties owed to their water contents being up to 38% and due to the presence of clay minerals. The Tenskinmeter Versus Skin (TVS) mud index has been developed following the concept of the *structure-surface* approach, based on the determination of the contact angle of Fomblin HC/25® Perfluoropolyether (PFPE) on mud surfaces. The TVS mud index is a very sensitive "surface tensiometry marker" capable of describing surface free energy variations of peloids during the maturation process. The level of the TVS mud index is based on the hydrophobic, lipophobic and self-repellent characteristics of Fomblin HC/25® Perfluoropolyether (PFPE). Owed to the repulsive forces generated at the interface between the substrate and Fomblin HC/25® Perfluoropolyether (PFPE), the TVS mud index has been used to define the quality, conformity, and the degree of maturation of thermal muds. The TVS mud index has also been demonstrated to evaluate the functional and therapeutic efficacy of a peloid. Considering the importance of pelotherapy in the modification of the selective permeability of skin, and consequently its influence on the hydration state of stratum corneum and on the permeation of therapeutic substances, this work describes the development of a surface tensiometry model for the assessment and optimisation of Japanese Biofango® mud therapy. This has been done through the evaluation of skin

*Corresponding author: e-mail: drossi@unite.it

hydration states before and after treatment with Biofango®, using water as a biocompatible test liquid, and determining the surface free energy of the used mud by implementing the Fomblin HC/25® Perfluoropolyether (PFPE).

Keywords: TVS mud index, euganean thermal muds, maturation process, contact angle method, mud therapy, skin hydration, biofango®

1 INTRODUCTION

Skin surface morphology and its softness, roughness, and surface profile have a great importance in many clinical and diagnostic applications [1]. The formation of scars on the surface of skin could give rise to clinical issues because the roughness of the surface influences the effectiveness of various therapies. For this reason, a non-invasive method for scar assessment, the Phase shift Rapid *In Vivo* Measurement of the Skin (PRIMOS), was developed to assess surface roughness of scars [2]. On the other hand, the morphologic study of skin has great importance for the evaluation of the stratum corneum (SC) and is a strong indicator of skin health, the formation of which depends mainly on its moisture level. Analytical techniques such as reflectance confocal scanning laser microscopy (RCSLM) are powerful tools to reveal the ultra-structure of the various skin layers [3] allowing one to determine the differences of refractive index between water, lipid, keratin, melanin, collagen and determining the condition of the stratum corneum (SC). The conditions of SC can be evaluated by analyzing the correlations between the cellular morphology and the moisture level of skin [3]. Other kinds of measurements such as transepidermal water loss (TEWL), electrical conductance, capacitance, impedance and other commonly applied methods like nuclear magnetic resonance, infrared, and Raman spectroscopies can reveal the water gradient of the SC [4]. The knowledge of the hydration state of skin is fundamental for the evaluation of the performance of personal care and wellness products which are strongly linked to the sliding friction behaviour of the SC which is dependent on the surface roughness [5]. The employment of a rotating ring-type measurement apparatus on the skin forearm proved that the friction coefficient (Ra) changes in relation to high skin hydration levels because the moisture of SC reduces the surface roughness, improves plasticity, and increases the real area of contact [5]. It is well known that the surface roughness of a substrate influences the evaluation of its wettability characteristics and is determined by the contact angle (CA: deg) method [6]. The relationship between roughness and wettability was defined in 1936 by Wenzel [6] who stated that the surface roughness enhanced the wettability caused by the chemistry of the surface and the substrates roughness ratio (r). From the results of Bloemen *et al.* [2], Leeson *et al.* [3] and Hendriks and Franklin [5],

it has been shown that there is a correlation between the hydration state of SC and the surface morphology of skin.

Since the 1990's some Authors have conducted extensive studies on the epidermic hydration using the contact angle method (CA; deg) [7]. This approach is called the "water on water" approach and was used to determine the wettability of skin with water, reducing the effect of surface roughness of SC on the CA measurement, and at same time utilized to determine its hydration state. This is confirmed by the fact that the measurement of skin roughness through profilometery revealed a significant linear relationship with skin dryness [8]. However, the effects due to the application of some products, such as hand lotion, on the wettability of skin have been studied previously [7]. Mavon *et al.* [9] investigated the surface free energy components of human skin, assessing the influence of skin lipids on surface wettability using advancing CA measurements of water, glycerol, formamide and diiodomethane. Mavon *et al.* [9] showed that skin surface lipids, mainly sebum, give the skin surface a hydrophilic characteristic. More recently, Elkhyat *et al.* [10] have shown that CA values, measured between the skin and mineral water, were smaller than those obtained between the skin and bi-distilled water prior to spring water (Saint GERVAIS) application. Elkhyat *et al.* [10] demonstrated that the skin hydration reduced the hydrophobia of the stratum corneum after the application of mineral water, showing a high affinity between the skin and the mineral water. These applications showed the feasibility to evaluate tensiometrically the skin moisture due to the presence of water on the SC which comes from both the transdermal evaporation and transpidermal water loss (TEWL). Following these works, in the 2000's the Tenskinmeter Versus Skin (TVS) test was developed, based on the surface tensiometry approach conducted by Mavon *et al.* [9] and Elkhyat *et al.* [10]. Differently from Mavon *et al.* [9], the TVS skin test is performed measuring the contact angle of a water drop deposited on skin surface. This method was preferred to the advancing contact angle method to obtain adhesion data not influenced by the application of external forces, but only by the gravity force. The TVS skin test accounts for the functional activity of natural and formulation systems and considers the relationship between the efficiency of the epidermic barrier of SC and the moisture of the skin [11]. The TVS skin test has also demonstrated the residual capacity of the epidermal cells to maintain their function as an epidermic barrier and their polarity due to the presence of water. The TVS skin test can also evaluate the capability of the epidermal cells to restore the SC architecture, keeping good functionality and an efficient epidermic state based on the degree of skin moisture [11]. With this in mind, TVS skin tests can be implemented to evaluate the moisturizing effect of a general formulation through the measurement of water CAs before and after the application of a properly prepared cosmetic formulation and/or natural systems such as Italian Euganean Thermal Muds (ETM) [12-14]. In this way, it is possible to evaluate the functional efficacies of these systems directly on a forearm's

skin, of which the surface appears smooth and with low roughness factor because of the water presence. In the case of peloids, the TVS skin test has shown that it is possible to evaluate the hydration effects of Euganean Thermal Muds (ETM) after the Mud Pack Treatment (MPT). Performed during the pelotherapy, these are commonly used in the spas of the Euganean Thermal Area (ETA) of Montegrotto and Abano Terme (PD-Italy) [11-14]. The ETM is a heterophasic natural system composed of a mineral component, thermal water and a biological component, deriving from the specific activity of the resident microflora [12, 13]. The contact and the combined action of these elements over time produce a visco-elastic and surface free energy evolutions and this time is generally termed the "maturation process". As a result, this can be studied through rheologic and surface tensiometry approaches [14]. Based on these considerations, more recently the surface free energies of ETM were evaluated in a non-destructive way, introducing a perfluoropolyether phosphate substance such as Fomblin HC/25® Perfluoropolyether (PFPEd) as the test liquid for surface tensiometry studies [15, 16]. Owed to the superhydrophobic, lipophobic and self-repellent properties of Fomblin HC/25® Perfluoropolyether (PFPE), and its low surface free energy (SFE=18.0 mN/m), PFPE was used to determine the quality and the maturation process of ETM by the contact angle method (TVS mud index) [17, 18]. The TVS mud index is based on the capability of Fomblin HC/25® Perfluoropolyether (PFPE) to sensitively and accurately evaluate peloids with different maturation process steps by using the contact angle method.

The HC/25® Perfluoropolyether (PFPEd) was also used together with diiodomethane and glycerine for the calculation of the dispersion component (DC; mJ/m^2), polar component (PC; mJ/m^2) and surface free energy (SFE; mJ/m^2) of ETM. The TVS mud index has been applied for the first time under monitoring activity on ETA's thermal muds, promoting new perspectives in the field of thermalism [19]. The HC/25® Perfluoropolyether (PFPEd) liquid test has also been used for the surface free energy characterization of conifers and their physiological growth, and raw coffee beans [20, 21]. In recent years, many foreign academic research groups and private companies have become interested in the study of thermalism such as Toho University (Tokyo, Japan) and the Japanese companies such as Ascendant Co. Ltd and Sanraku-en spa Ryokan (Tonami – Japan) who introduced the pelotherapy in association with other more traditional thermal treatments [22-24]. The Sanraku-en Spa Ryokan (Tonami, Toyama, Japan) has started to implement the "Shogawa biofangotherapy" with the aim to develop a new therapeutic protocol [22]. Shogawa uses hot spring water and different varieties of clay of natural origin (called Biofango®). The clay-containing muddy matrices are matured with hot spring water for three weeks during which bacterial flora develops, with the production of constitutive elements having therapeutic properties. The Ascendant Co. Ltd developed the production of the first Japanese Biofango® in collaboration with Sanraku-en Spa Ryokan, Toho University (Tokio –

Japan), University of Science and Technology of Hokuriku (Japan), and Jaist of University of Hishigawa (Japan). The formation of biofango® opened a new perspective in pelotherapy for therapeutic use in Japan. This new thermal project is known as the "Biofango® project" and demonstrated that the contact between the hot spring water and Biofango® could produce a biological maturation process [22]. The Japanese style "fango" can be produced by using hot spring water of Yugawara Hot Spring (Hakone Hot Spring Area, Kanagawa Prefecture) and specific microbiological means. Microbiological studies were performed while making fango using the original hot spring water [25, 26]. These studies confirmed the presence of thermophilic bacteria (No527) in Japanese Yugawara Hot Spring water at 59°C and pH 8.09. Following these studies, the Biofango® project enriched itself with many contributions of research performed with the traditional Italian thermalism [25-26]. Considering these studies, this research work develops a surface tensiometry method for the evaluation of the hydration effects of an artificial Japanese Biofango® after a complete treatment on subjects of different ages, sex and weights, evaluating and optimizing the "Biofangotherapy" mudtherapy protocol which is being applied in Sanraku-en Spa Ryokan. For this purpose, a simple method has been developed for the evaluation of the hydration performance of Japanese Biofango® through TVS skin tests. This has been done through the development of a new surface tensiometry method for the characterization of the surface free energy of used Biofango® after the implementation of the mud therapy protocol using the TVS mud index.

2 EXPERIMENTAL TECHNIQUE

2.1 Materials

2.1.1 Biofango® mixtures

The Japanese Biofango® BFM, used for mud therapy, was constituted by Kunigel, Kaolinite, and Wakura Diatomite, containing montmorillonite with good moulding performance. The mineral composition of Biofango® BFM mixtures compared with the other mixtures prepared by Marukoshi Co. Ltd is shown in Table 1.

Figure 1 and Table 1 shows the X-ray diffraction data of the Japanese clays used in the Biofango® mixtures. Table 2 provides the X-ray fluorescence (XRF) profile of the Wakura Diatomite and Kaolinite components employed in Biofango® BFM. The ETM contained *calcite (CaCO3)* and *dolomite* but Japanese Biofango® contained only small traces. The ETM was crystalline and contained a large amount of *Calcium-carbonate (CaCO3)* and *Magnesium-carbonate*. The mixture A01 (KasaokaBentonite 1.25 Kaolinite 0.5 Diatomite 0.25) had good physical characteristics for topical applications. Biofango® BFM was collected in triplicate from a Sanraku-en maturation plant following the sampling method developed in OTP. Samples were placed

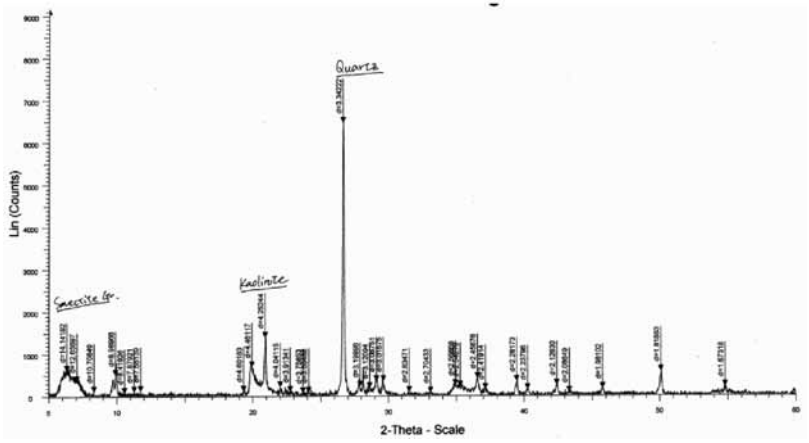

FIGURE 1
X-rays diffractometry (XRD) profile of Japanese Biofango® (BFM).

TABLE 1
Japanese Biofango® mixtures.

	Benton-ite			**Clay**			**Diato-mite**	**Carbonate**		**Sil-ica**	**%**
Type	Kunigel V1	Kasa-oka	Asama	Neo-clay	NN Kaolin	Hon-yama	Wakura	Dolo-mite	Cal-cite	Sil-ica	T/L
BFM	70				20		10				100
MAT1		60		5		10	10	10		5	100
MAT2	30					32	10	18		10	100
MAT3				30		15	10	35		10	100

inside of 20 ml PE-HD containers equipped with a stopper and under stopper and stored at –25 °C in controlled conditions before analysis. The degree of swelling differed and follow the order of gradient: Kasaoka < Asama < KunigelV1 = Neoclay (Table 1).

2.1.2 Determination of surface energy free energy (SFE) of used Biofango® (BFM)

The test liquids used for the development of the surface tensiometry method, for surface free energy (SFE; mJ/m^2) characterization of the used Biofango® (BFM), was carried out in accordance with what was established for the Euganean thermal mud (ETM) of the Euganean Thermal Area (ETA) (18). Glycerol %98, Fomblin HC/25® Perfluoropolyether (PFPEd) (SFE=18.1 mN/m, DC=18.0 mN/m, PC=0.1 mN/m) from Kalis srl (Cornuda, Italy), diiodomethane (dim)

TABLE 2
X-ray fluorescence (XRF) profile of components used for the formulation of Biofango® mixtures.

Raw material	SiO2 (%)	Al2O3 (%)	Fe2O3 (%)	TiO2 (%)	CaO (%)	MnO (%)	K2O (%)	Na2O (%)	Ig.Loss (%)	Mineral assemblages
Komatsu clay	53.38	31.49	0.91	0.53	0.20	0.20	1.90	0.19	11.80	Kaolinite-Quartz-Feldspar
Motoyama clay	48.86	34.22	1.32	0.89	0.15	0.24	0.85	0.04	13.32	Quartz-Montmorillonite-Feldspar-Carbon
Wakura diatomite	78.20	10.60	4.42	0.49	1.00	1.31	1.70	0.96	12.20	Quartz-Montmorillonite-Feldspar-Grauconite
Kasaoka bentonite	66.01	16.90	5.36	-	0.87	0.70	2.82	1.35	5.19	Montmorillonite-Quartz-Feldspar-Christobalite

(SFE=50.8 mN/m, DC=50.8 mN/m, PC=0.0 mN/m) from Acros Organics (New Jersey, USA) and Fomblin HC/OH-1000® Perfluoropolyether (PFPEd2) from Kalis srl (Cornuda, Italy) were used for the determination of the surface free energy of used BFM. In particular, PFPEd2 has a fluorocarbon chain formula $HO\text{-}CH_2CF_2O\text{-}(CF_2CF_2O)_p\text{-}(CF_2O)_qCF_2CH_2\text{-}OH$ (where $p/q=0.5\div3.0$), and was characterized using un-treated titanium (TI) (SFE=39.5 mN/m, DC=11.4 mN/m,PC=28.2 mN/m) (3T; Perugia, Italy), such as that reported by Aeimbhu [27], un-treated stainless steel Cr-Ni AISI 314 (ST) (SFE=43.4 mN/m, DC=24.6 mN/m, PC=18.8 mN/m), such as that reported by Bortolozzi *et al.* [28] with smooth cell wall surfaces and few irregularities, and alluminium (AL) (SFE=38.1 mN/m, DC=25.3 mN/m, PC=12.8 mN/m), with compact and a less random un-treated surface such as the aluminium alloy reported by Leena *et al.* [29] , as test solids. Figure 2 shows the SEM analyses of the surface of TI. The number of droplets of Fomblin HC/25® Perfluoropolyether (PFPEd) deposited on the surface of the test solids were three (N=3). The test solids listed above were previously characterized by the contact angle method (CA; deg) using water mQ (WmQ), Fomblin HC/25® Perfluoropolyether (PFPEd), and Ethylen glycole (EG).

2.1.3. Determination of skin hydration and surface free energy (SFE) of exhaust BFM

Skin hydration analysis was carried out before and after treatment with BFM using WmQ (15MΩ*cm) from the Department of Pharmaceutical and Pharmacological Sciences (University of Padova, Italy), and employing Tensiometer (Tenskinmeter®) (MobilDrop DSA 2; Krüss, Hamburg, Germany) (see Figure 3a). The Tenskinmeter® is a MobilDrop DSA2 tensiometer with a Teflon support for skin surface applications (see Figure 3b). One water droplet was used for CA measurements for each Sanraku-en thermal protocol.

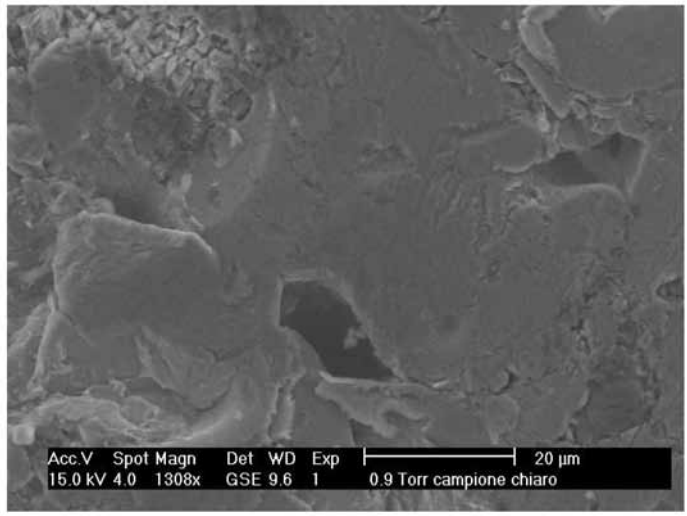

FIGURE 2
SEM analysis of untreated TI flat surface (1300x).

FIGURE 3
MobilDrop DSA2 (by Krüss - Hambourg – Germany) and Tenskimeter with Teflon support for skin applications (Courtesy of Development Cooperation BAZH.I - NGO, Maserada Sul Piave, Treviso, Italy).

The SFE of used BFM mixture was measured using a Static Tensiometer (DSA 10; Krüss, Hamburg, Germany) supplied with 20 µl syringes and a blunt needle with a diameter, ϕ, of 0.5 mm (see Figure 4). Both Tensiometers were supplied with software DSA provided by ENCO srl (Spinea, Italy).

FIGURE 4
Static DSA 10 Surface tensiometry Unit (STU) in Sanraku-en spa (Tonami – Japan 2010).

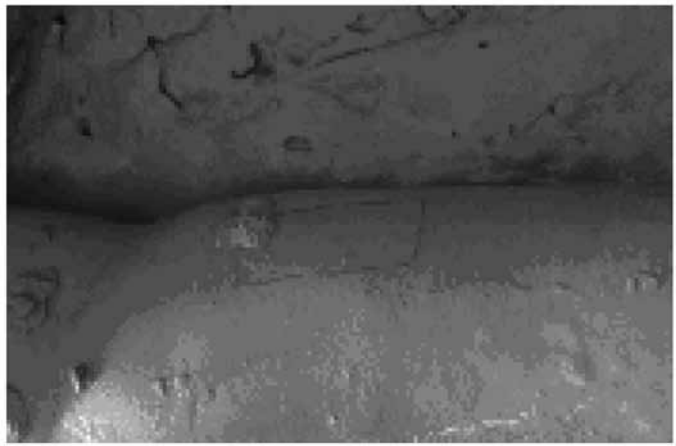

FIGURE 5
Biofango® (BFM) mudprint at skin interface.

3 EXPERIMENTAL METHODS

3.1 Sampling of Biofango® BFM

Sampling was performed by collecting used Biofango® BFM from the mudprint left on the arm skin after the mud therapy phase of the Sanraku-en mud therapy protocol. Muddy matrices were put in PE-HD containers and stored in freezing conditions at –25 °C (see Figure 5).

3.2 Determination of surface energy free energy (SFE) of exhaust BFM

The Owens-Wendt (OW) model [30] was used to determine the SFE of the BFM Biofango® mixtures. The OW model is based on the Young's equation (see Equation 1).

$$\gamma_{SL} = \gamma_S - \gamma_L \cos\theta \quad [1]$$

where γS is the total surface free energy of systems, γSL is the interfacial tension between systems and liquid, γL is the surface tension of the liquid, and θ is the apparent contact angle measured at the equilibrium point (see Equation 2) after 0.5s from the contact between the liquid test and the surface of the system (N=3) [30-32].

$$F(\gamma s,\gamma l,\gamma sl) = 0 \quad [2]$$

The total surface free energy γ is divided into a dispersed () and polar () component according to the formula. The interfacial tension between a solid and a liquid is evaluated by the geometric mean (see Equation 3).

$$\gamma_{SL} = \gamma_S + \gamma_L - 2\sqrt{(\gamma_S^d \gamma_L^d)} - 2\sqrt{(\gamma_S^p \gamma_L^p)} \quad [3]$$

with dispersed(γ_L^d) and polar (γ_L^p) components of the liquid and dispersed (γ_S^d) and polar (γ_S^p) components of the solid. Combining the two previous equations, two linear equations can be provided (see Equation 4a and 4b).

$$x + ay = b(1 + \cos\theta_1) \quad [4a]$$

$$x + cy = d(1 + \cos\theta_2) \quad [4b]$$

Where the intercept, x, is $\sqrt{\gamma_S^d}$ and the slope, y, is $\sqrt{\gamma_S^p}$,corresponding respectively to the square roots of dispersion and polar components. This makes it possible to assess the two unknown components of the SFE for the solid [33].

3.3 Determination of CA of Fomblin HC/25® Perfluoropolyether (PFPEd) by Fast Contact Angle Method (FCAM).

The measurement of the contact angle between PFPEd (where "d" is defined as drop) was performed considering the best compromise between the sharpness (relative focus value; >1 pixel) of the image of the drop deposited on the surface and the time during which the picture is taken (<0.5s) (see Equation 5).

$$f = \frac{S(px)}{t(s)} \quad [5]$$

where f is a dimensionless pure number that represents the CA measured, S is the image sharpness (px), and t (s) is the "snapshot" time of image. The f parameter could change in relation to the kind of solid substrate analyzed. The parameter f was developed by the Fast Contact Angle Method (FCAM). Ideated by the Author, the FCAM is the method of PFPEd contact angle measurement used for the development of the Tenskinmeter versus skin (TVS) mud index [18]. As PFPEd was introduced for the first time in surface tensiometry by the Author for the characterization of the surface free energy of solid substrates by FCAM method, the parameter f was named The Rossi factor.

3.4 Determination of skin hydration by contact angle method

Hydration analysis of the skin was carried out in a simplified way by implementing the static contact angle method (CA; deg), measuring the CA of a single droplet of water at the equilibrium point (Equation 2) after 0.5 s. This was carried out on the skin before and after treatment with Biofango® and in accordance with the traditional Sanraku-en/Biofango® protocol. Aiming to develop a method for assessing the hydration effect after a complete thermal treatment with "Sanraku-en/Biofango® protocol", four subjects with different ages, sexes and weights (KS, YS, MO, and KM) were considered as test subjects (see Figure 6).

3.5 The Sanraku-en Biofango® mudtherapy protocol

The Sanraku-en mudt herapy protocol was composed of three phases; (a) bath therapy (8'), (b) mud therapy (20'), and (c) shower (3') (see Figure 7).

FIGURE 6
Skin hydration measurements before (a) and after (b) treatment with "Biofangotherapy"

FIGURE 7
Typical Sanraku-en protocol phases: (a) baththerapy (8'), (b) mudtherapy (20'), (c) shower (3').

FIGURE 8
Blood pressure measurement before and after "Biofangotherapy"

3.5.1 Evaluation of Sanraku-en mudtherapy protocol by surface tensiometry approach

Surface tensiometry evaluation of the mud therapy protocol was based on the Sanraku-en mud therapy phases composed by the following steps: (a) blood pressure measurement of the patient (see Figure 8), (b) evaluation of the skin hydration measuring water contact angles on the left and the right arm before treatment, (c) thermal bath treatment (8'), (d) skin hydration evaluation after the thermal bath, (e) BFM mud therapy (20'), (f) evaluation of skin hydration after the BFM mud therapy on the left and the right arm, (g) shower (3'), (h) evaluation of skin hydration after the shower, and (i) blood pressure measurement after the end of protocol.

3.5.2 The dr-Biofango® Protocol Method (dr-BPM)

The dr-Biofango® Protocol Method (dr-BPM) was developed to get a personalized surface tensiometry profile of skin hydration of the test subjects at the end of each phase of the treatment protocol. The dr-BPM diagram aimed to assess the moisture content of the skin after each phase of treatment in relation to the hydration state of the BFM mud applied.

The test liquids, detailed previously, and glycerol, were used respectively for the analysis of the wettability of skin and BFM. These liquids were chosen because of their capability to determine the water presence on biologic, natural and formulation systems. The variation of skin hydration was calculated by considering the moisturizing state of BFM before the treatment and its hydration contribution (see Equation 6).

$$\Delta^{W}(\text{deg}) = CA_{gly}^{BFM}(\text{deg}) - [(CA_{WmQ}^{Skin(r)}(\text{deg}) - CA_{WmQ}^{Skin(l)}(\text{deg})] \qquad [6]$$

where Δ^{w} represents the variation of the skin hydration state measured at the end of Biofango® therapy, represents the glycerin CA value measured on the surface of BFM (reference value 17.09 deg) before the mud therapy protocol (basal), and represents the water CA measured on the right forearm and left forearm, respectively. The same calculation was performed after the bath therapy and shower phases. Equation 6 led to the characterization of the different levels of hydration between BFM and the epidermis at the end of mud therapy phase and the levels of skin moisturize after bath and shower phases, in relation to the hydration effect and functional efficacy of BFM.

4 RESULTS

4.1 Determination of hydration state of skin by dr-Biofango® Protocol Method – dr-BPM

The measurement of the CA of water on the skin surface of subject KS showed elevated values before (t_0>89.5 deg) and after (t_f>89.5 deg) treatment, while there was a marked decrease in blood pressure (see Table 3). The values relating to the hydration of the skin after treatment showed no significant changes. Based on these first results, a wettability analysis was performed on the skin of three more test subjects (KM, YS, MO) to evaluate the changes of the hydration of their epidermis at the end of each phase of the Sanraku-en/Biofango® protocol (see Table 4).

The data in Table 5 shows a low skin hydration of subject YS followed by a great increase of the values only after treatment with BFM (basal values).

TABLE 3
Water contact angles values measured on skin of KS test subject (deg) and blood pressure parameters (mmHg).

Time (min)	**Water contact angle (deg)**		**Blood pressure (mmHg)**
	left	right	min
t_0	96.8	90.0	87.0
t_f	90.0	95.0	87.0

TABLE 4
Scheme of skin hydration evaluation for KS test subject.

BATH	Water contact angles (deg)		Blood pressure (mmHg)	
	left		right	min
t_0	96.8	90.0		87.0
t_f	-	-		-
MUD	**Water contact angles (deg)**		**Blood pressure (mmHg)**	
	left		**right**	**min**
t_0	-	-		-
t_f	-	-		-
SHOWER	**Water contact angles (deg)**		**Blood pressure (mmHg)**	
	left		**right**	**min**
t_0	-	-		-
t_f	90.0	95.0		87.0

After the shower, the subject quickly lost the moisture content acquired during the Biofangotherapy and showed higher levels of CA pf water, closer to those measured at the end of the thermal bath.

Figure 9 shows the dr-BPM diagram of subject YS. In this case the CA demonstrated to be out of the range of acceptability of the OW model. The calculation of D^w links the hydration state of the skin measured by the CA method with the hydration efficacy of mud therapy operated with BFM, bath, and shower phases (see Figure 10). The grey area represents the differences between the skin hydration and the moisturizing efficacy of the mud therapy, bath, and shower phases. Considering this, the larger area shows the hydration effects of the Sanraku-en protocol phases. After the Biofangotherapy phase (mud therapy), there was an increase in the hydration state of the skin due to the high presence of water pres-

TABLE 5
Normal scheme of skin hydration evaluation for YS test subject.

BATH	Water contact angles (deg)		Blood pressure (mmHg)
	left	right	min
t_0	120.0	124.4	79
t_f	98.50	104.0	-
MUD	**Water contact angles (deg)**		**Blood pressure (mmHg)**
	left	**right**	**min**
t_0	98.5	104.0	-
t_f	40.6	39.90	-
SHOWER	**Water contact angles (deg)**		**Blood pressure (mmHg)**
	left	**right**	**min**
t_0	40.6	39.9	-
t_f	90.7	90.4	76

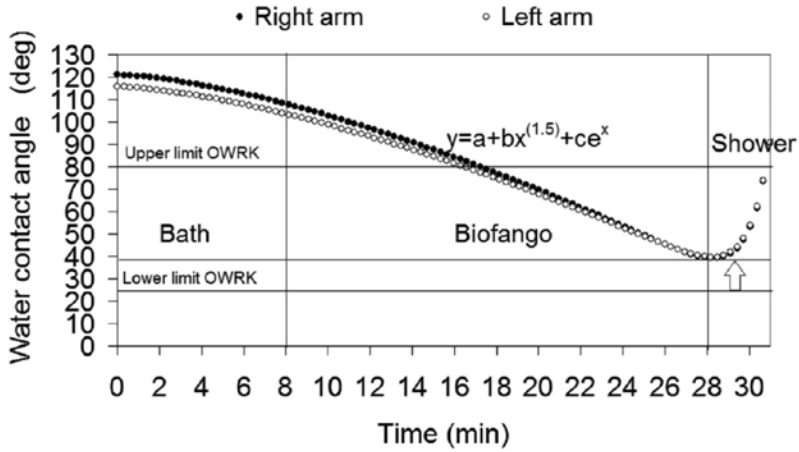

FIGURE 9
Personalized dr-BPM diagram for YS test subject. The blue arrow indicates the hydration needs of the skin (CA>24.8 deg).

ent in the BFM. The small values of D^w measured at the end of the Biofango-therapy, and the negligible effects of the bath and the shower phases on skin hydration, demonstrated that a large part of the moisturized effect of the mud therapy was lost in a short time. Based on the diagram of the dr-BPM of subject

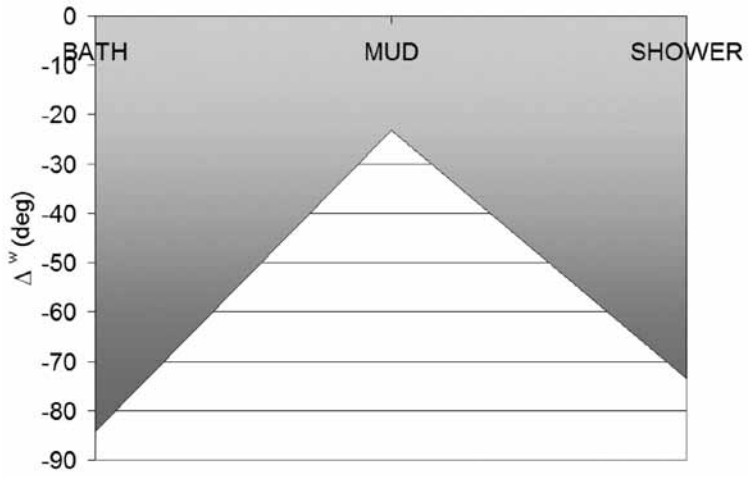

FIGURE 10
Variation of skin hydration of YS test subject (D^W) due to the hydration effect of BFM on skin of YS test subject test after "Biofangotherapy"

YS (see Figure 8) and to improve, as much as possible, the moisturizing effect of the treatment with BFM, it was proposed to reverse the Sanrakuen/Biofango® protocol exchanging timely the bath phase with the Biofango® therapy step (modified protocol Sanraku -en/Biofango®). The greater moisturizing effect obtained after applying the BFM was witnessed by the lower values of CA of water measured at the interface with respect to the skin (see Table 6).

The dr-BPM diagram shows the trends and behaviours of water CAs outside the acceptability range of the OW model at the end of bath therapy (20'), and after the shower phase (left forearm). These two results confirmed that it is possible to optimize the moisturizing effects of BFM for subject YS after a personalized modification of the classic Sanraku-en/Biofango® protocol (see Figure 11).

The behaviour of the skin hydration showed that, after the completion of the Sanraku-en protocol, the best hydration effect at the skin/BFM interface was reached earlier than the time needed in the traditional Sanraku-en/Biofango® protocol. Consequently, an increase of the moisturizing effect at the end of BFM treatment occurred and corresponded with the decrease of the bath-mud-shower area (grey area) (see Figure 12). The increase of D^w values for bath and shower phases were due primarily to the positive influence of the mud therapy phase on the skin hydration. It is hypothesized that the increase of the hydration effect of BFM could impact on the other two phases and also reduce the loss of skin moisture.

The data reported in Table 7 shows a reduction of the basal values of skin hydration followed by a marked increase after the treatment with BFM during the normal Sanraku-en mud therapy protocol applied to test subject MO.

TABLE 6
Inverted scheme of skin hydration evaluation for YS test subject.

BATH	**Water contact angles (deg)**		**Blood pressure (mmHg)**
	left	**right**	**min**
t_0	108.4	112.0	79
t_f	28.0	32.8	-
MUD	**Water contact angles (deg)**		**Blood pressure (mmHg)**
	left	**right**	**min**
t_0	28.0	32.8	-
t_f	83.7	91.2	-
SHOWER	**Water contact angles (deg)**		**Blood pressure (mmHg)**
	left	**right**	**min**
t_0	83.7	91.2	-
t_f	85.1	89.36	76

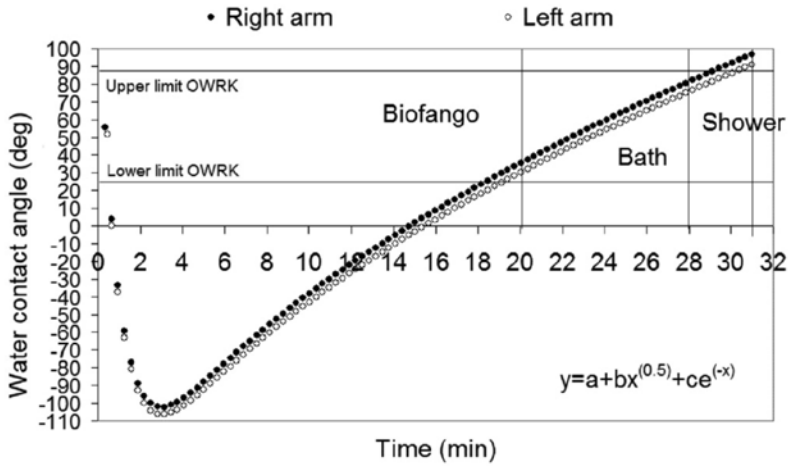

FIGURE 11
Personalized dr-BPM diagram for YS test subject after the inversion of Sanraku-en phases.

After the shower phase, subject MO very quickly lost the moisture content acquired during the Biofangotherapy showing higher levels of water CAs, but still lower with respect to the CAs measured at the end of the bath phase.

In the case of the MO test subject, the dr-BPM gave rise to a satisfactory moisturizing effect compared to the traditional type of Sanraku-en/Biofango® protocol

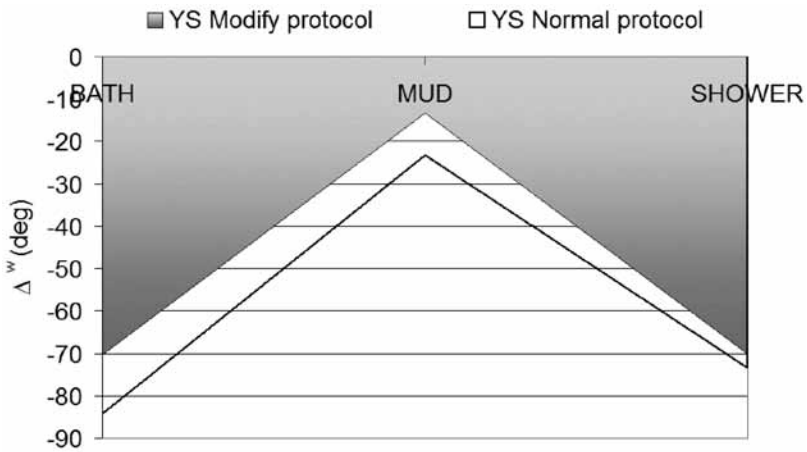

FIGURE 12
Variation of skin hydration of YS test subject (D^W) due to the hydration effect of BFMperformed after the inversion of "Biofangotherapy" phases (Modify protocol) respect to normal protocol.

TABLE 7
Scheme of skin hydration evaluation for MO test subject.

BATH	**Water contact angles (deg)**		**Blood pressure (mmHg)**
	left	**right**	**min**
t_0	108.7	100.4	87
t_f	98.5	104.0	-
MUD	**Water contact angles (deg)**		**Blood pressure (mmHg)**
	left	**right**	**min**
t_0	98.5	104.0	-
t_f	21.7	18.6	-
SHOWER	**Water contact angles (deg)**		**Blood pressure (mmHg)**
	left	**right**	**min**
t_0	21.7	18.6	-
t_f	78.6	86.0	87

(see Figure 13). This result shows that the inversion of the phases of the Sanraku-en thermal protocol is not required for the test subject under consideration.

The comparison between the hydration effects of BFM after the treatment of test subjects, MO and YS, with traditional protocol, and the same YS test subject treated with the inverse Sanraku-en protocol, demonstrated that the moisturizing effects of mud therapy is higher for subject MO than subject YS

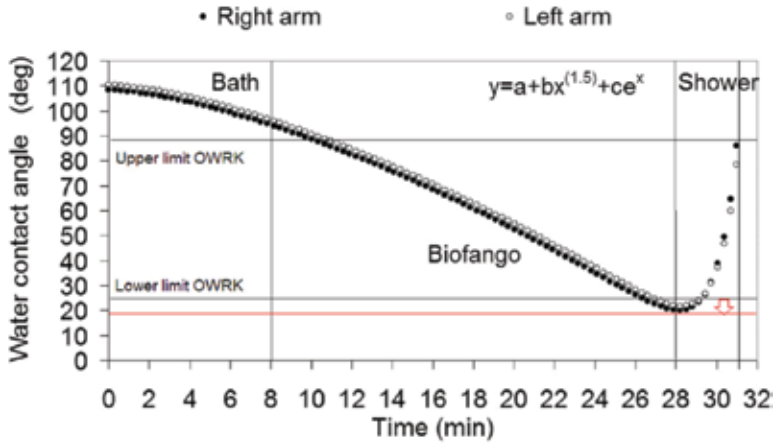

FIGURE 13
Personalized dr-BPM diagram for MO test subject where the red arrow shows the increase of hydration state after treatment with Sanraku-en protocol (CA< 24.8 deg).

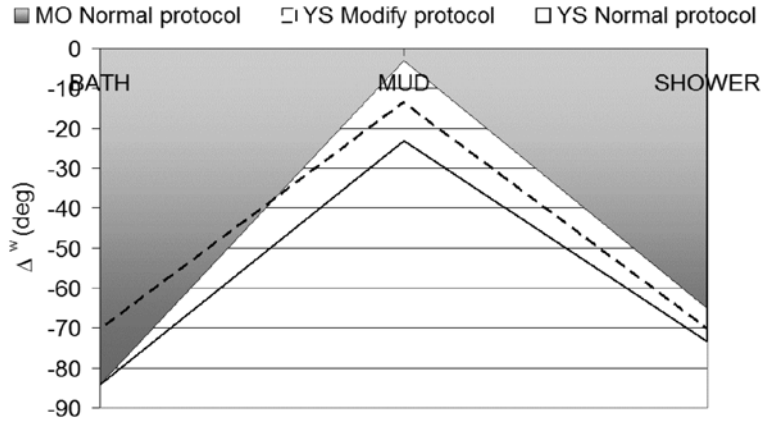

FIGURE 14
Comparison between the variation of skin hydration (D^W) of MO test subject after the treatment with BFM and that of YS test subject after the application of normal and inverse Sanraku-en mud therapy protocol.

(see Figure 14). The bath-mud-shower area (grey area) related to subject MO appearing less wet than the other cases, confirming the influence of the significant variables on the hydration state after Biofangotherapy.

In the case of fourth test subject KM, the data in Table 8 shows that a reduction of the basal values of skin hydration with an increase of its moisture only after the treatment with BFM. In this case, test subject KM had quickly lost the moisture content acquired during the Biofangotherapy, show-

TABLE 8
Scheme of skin hydration evaluation for KM test subject.

BATH	**Water contact angles (deg)**		**Blood pressure (mmHg)**
	left	**right**	**min**
t_0	109.0	108.3	94
t_f	104.0	115.2	-
MUD	**Water contact angles (deg)**		**Blood pressure (mmHg)**
	left	**right**	**min**
t_0	104.0	115.2	-
t_f	34.8	47.8	-
SHOWER	**Water contact angles (deg)**		**Blood pressure (mmHg)**
	left	**right**	**min**
t_0	34.8	47.8	-
t_f	90.5	101.0	92

ing higher levels of water CAs closer to those measured at the end of the bath phase (see Figure 15). The comparison between the dr-BPM diagrams for all test subjects demonstrated the lowest moisturizing effects of BFM on test subject KM (grey area) whose bath-mud-shower area was larger than that of YS (normal protocol), YS (inverse protocol) and MO (normal protocol) (see Figure 16).

4.2 Determination of the Surface Free Energy (SFE) of exhaust BFM

The CAs of test liquids measured on BFM before and after the cutaneous application are reported in Table 9. After the application of BFM on the forearm skin of the test subjects, the surface tensiometry parameters SFE, DC, PC, CA, and TVS mud index (CA of PFPEd) of BFM were determined before (basal t_0) and after the treatment (t_f) (see Figure 17).

Figure 17 shows that during the treatment the BFM DC decreased (increase of TVS mud index values) maintaining its PC (test subject KM), DC decreased (increase of CAs of dim and TVS mud index levels) and maintained its PC (test subject MO), DC decreased (decrease of CAs of dim and TVS mud index levels) keeping stable its PC (test subject YS after normal Sanraku-en protocol), with all of the surface free energies remaining at the basal level (test subject YS after inverse Sanraku-en protocol), and DC decreasing after the treatment of test subject KS (decrease of CAs of glycerine).

After the inversion of Sanraku-en protocol, the BFM didn't change significantly as the levels of SFE, DC and PC were more stable with respect to

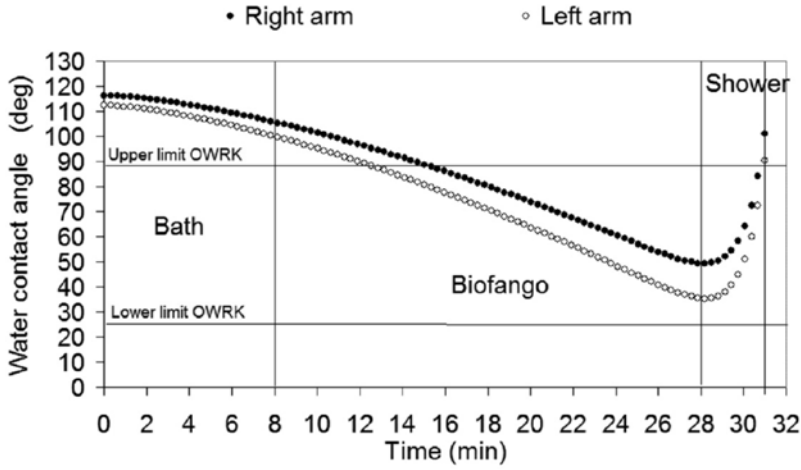

FIGURE 15
Personalized dr-BPM diagram for KM test subject.

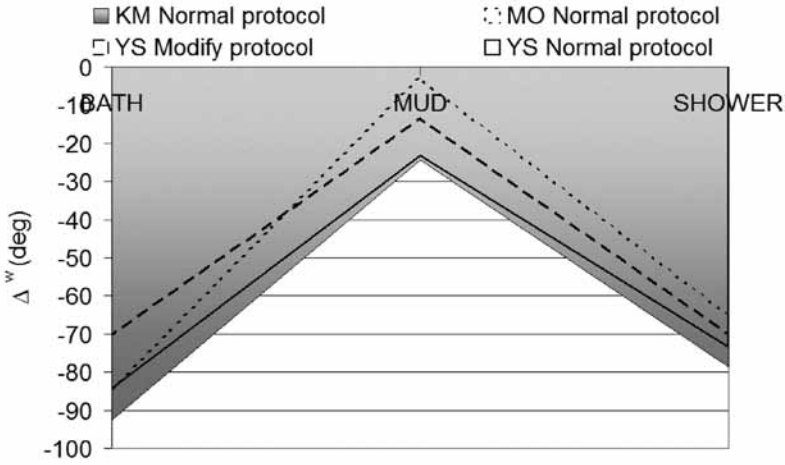

FIGURE 16
Comparison between the variation of skin hydration (D^W) of KM, , YS (normal protocol), YS (inverse protocol), and MO test subjects after treatment with BFM.

the other test subjects. It is hypothesized that the increase of skin hydration of test subject YS observed after the inversion of the protocol could be due to the "barrier effect" of the BFM. The BFM therefore appears capable of keeping its surface free energy components after the first step of the mud therapy protocol.

TABLE 9
CA of glycerol (gly), Fomblin HC/OH-1000® Perfluoropolyether (PFPEd2) and Fomblin HC/25® Perfluoropolyether (PFPEd) liquids test measured on the surface of BFM mud before (t_0) and after (t_f) the treatment of subjects tests KS (CA^{KS}: deg), MO (CA^{MO}: deg), YS (CA^{YS}: deg), YS after the inversion of Sanraku-en mudtherapy protocol ($CA^{YS\ INVERSE}$: deg) and KM (CA^{KM}: deg).

Liquids	CAKS(deg)		CAMO(deg)		CAYS(deg)		CAYS INVERSE(deg)		CAKM (deg)
test	t0	tf	t0	tf	t0	tf	t0	tf	t0
Gly	17.1±5.4	14.2±0.3	17.1±5.4	18.3±6.8	17.1±5.4	21.2±0.3	17.1±5.4	17.0±10.7	17.1±5.4
PFPEd2	57.4±1.4	56.3±1.2	57.4±1.4	30.3±1.7	57.4±1.4	39.3±2.4	57.4±1.4	24.7±3.2	57.4±1.4
PFPEd	44.9±1.5	30.4±0.9	44.9±1.5	67.1±3.7	44.9±1.5	51.0±3.8	44.9±1.5	61.6±3.7	44.9±1.5
OWRK model									
R^2		0.824		0.90		0.85		0.89	

The relationship between TVS mud index and DC is shown in Figure 18 and confirmed the great reduction of DC, of the BFM, after its application on test subjects, MO and KM. After the Biofango® BFM and shower phases, test subject MO reached its highest skin hydration showing water CAs under the two OW limits (see Figure 19), and consequently the hydration efficacy of BFM led to a satisfactory moisturizing effect using the traditional Sanraku-en/Biofango® protocol. In the case of YS and KM, the water CA levels after BFM treatment appeared to be at the lower OW limits, and consequently the skin hydration was not satisfactory (see Figure 19). For this reason, the test subjects YS and KM underwent a second treatment with the same BFM but inverting the Sanraku-en/Biofango® protocol. The inversion of protocol led to an improvement of the hydration state of the skin of YS test subject after the treatment with BFM (20').

The positive effect of the inverted Sanraku-en/Biofango® protocol in the optimisation of the hydration level of YS skin (D^{CA}) is showed by the decrease of the water contact angles levels after 20'. Due to the inversion of the protocol, the water CAs became closer to the lower OW limit (24.8 deg). As physiological parameters of correlation, the heart rate differences of each test subject were considered and recorded at the end of each treatment protocol (see Equation 7). In a similar manner, the water CA differences were measured on the right and left forearms skin at the end of each phases also. To measure the kind of correlation between surface tensiometry and physiologic data, an equation for the calculation of the water CA differential between right and left forearm was developed (see Equation 8).

$$\Delta^{HR} = n_f - n_b \qquad [7]$$

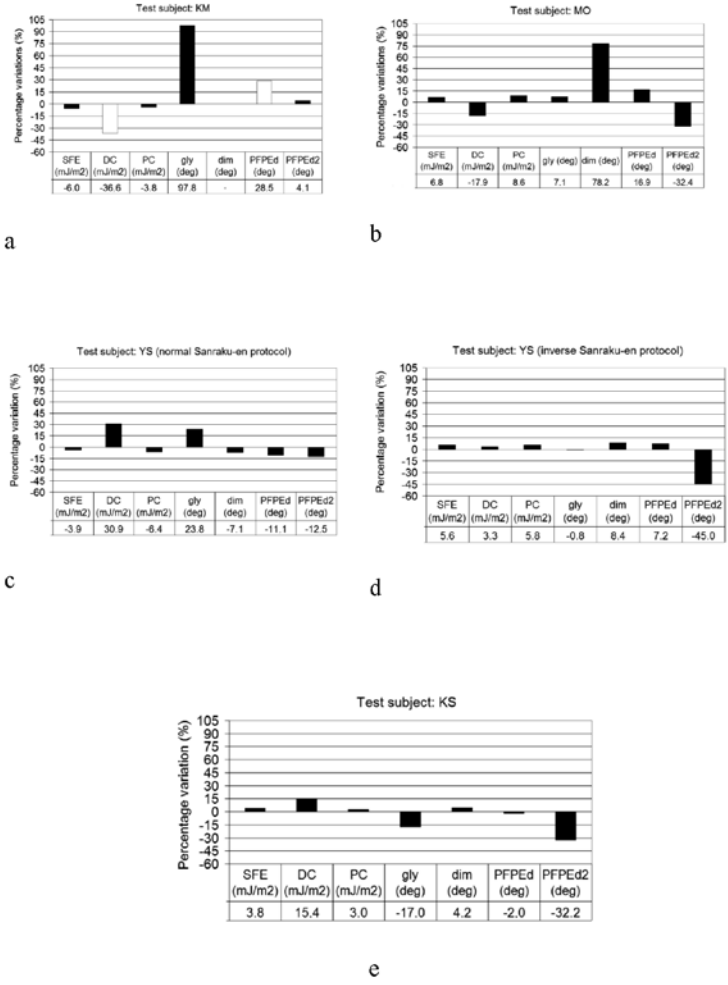

FIGURE 17
Variations of surface free energy parameters of BFM mud after (t_f) the application of Sanraku-en protocol on forearms skin of test subjects (exhaust/used BFM).

$$\Delta^{CA^{r/l}_{skin}} = \left| \frac{\sum_{i=1}^{4} \left(CA^{skin(r)}_{WmQ} - CA^{skin(l)}_{WmQ} \right)_i}{n} \right| \qquad [8]$$

where Δ^{HR} is the heart rate differential, n_f is the number of rate measured after Sanraku-en/Biofango® treatment, n_b the number of rate measured before Sanraku-en/Biofango® treatment, the water contact angles differential between right and left forearm, the water contact angles values measured on right arm,

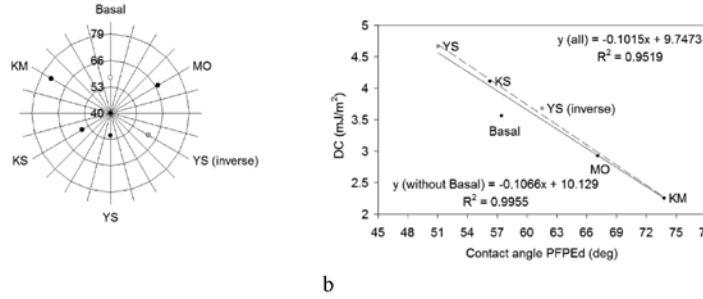

FIGURE 18
TVS mud index levels of exhaust (used) BFM collected from MO, YS, KS, and KM test subjects skins (17a), and correlation between CA (deg) of Fomblin HC/25® Perfluoropolyether (PFPEd) (performed by FCAM) and dispersion component (DC; mJ/m^2) of exhaust (used) BFM fango and the effect of basal BFM on the coefficient of correlation (R^2) (17b).

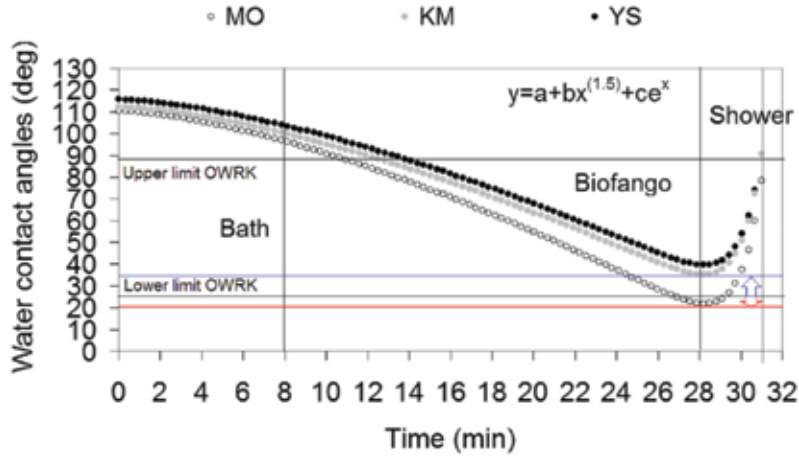

FIGURE 19
Comparison between dr-BPM diagrams of MO, KM, and YS (treated with BFM using normal protocol) test subjects, where the red arrow indicates the good hydration state of MO skin (CA<24.8 deg) and the blue one the hydration needs of the skins of the other test subjects (CA>24.8 deg).

the water contact angles values measured on left arm, and n (n=4) the number of determinations corresponding to the phases of Sanraku-en protocol (basal, bath, pelotherapy, shower). Figure 21 shows the correlation between the surface surface tensiometry parameters () and physiological data [$y=\sqrt{(e^{\Delta HR})}$].

Figure 21 shows that the Δ^{HR} and were well correlated (R^2=0.997). As an example, test subject KM demonstrated high numbers of beats for minute

measured before the treatment and a greater decrease in heart rate measured at the end of protocol than the other two test subjects. This wide variation appeared to correspond to an equally large difference between the average values of water CAs measured between right and left skin's forearms. Test subject YS presented minor differences in the number of heart pulses after treatment that could be linked to low changes in water CAs. In the end, test subjects, MO and KS, showed negligible differences in both surface tensiometry and physiological data.

In accordance with Equation 5, the analysis of the correlations between the glycerol's CAs measured on the surface of BFM, and the water CAs measured on the skin surface before and after treatment, demonstrated the real hydration capability of BFM (see Figure 22a). The analysis of the correlations between glycerol's CAs and Δ^{HR} values confirmed the link existing between surface tensiometry (CA; deg) and physiological (HR; b/min) parameters in relation to the hydration efficacy of BFM (see Figure 22b).

In the end, the correlations reported in Figure 22a showed a strong relationship between the CA of water measured on the forearm of test subjects KS, MO, YS, KM, their heart rate, and the hydration state of BFM determined by the measurement of the CA of glycerol. Figure 22b demonstrated good correlation between the wettability of BFM with test liquids more polar such as glycerol (R^2=0.95) and Fomblin HC/OH-1000® Perfluoropolyether (PFPEd2) (R^2=0.87), and the physiological parameter Δ^{HR}, confirming the interconnections between the skin hydration and the heart rate (see Figure 21)

Figure 23a confirmed the influence of the polar components (PC; mN/m) of glycerol and Fomblin HC/OH-1000® Perfluoropolyether (PFPEd2) on the correlation between CA measured at water/skin interface and gycerine (R^2=0.97), and with the same perfluoropolyether (R^2=0.90). Figure 23b demonstrated also a good correlation (R^2=0.76) between the SFE (mJ/m^2) of BFM and the CA (deg) of water measured on the skin surface of each test subject.

5 DISCUSSION

The low hydration state of the forearm skin of test subject KS was proved by the analyses of the CA of water (see Table 3) and the study of the variations of SFE, DC, PC, and CA of BFM (see Figure 17). The rapid loss of the moisturizing effect of BFM observed in Figure 9 after biofango® skin application appeared in accordance with the increase of DC and decrease of PC of the peloid occurred after the treatment of test subject YS using the traditional Sanraku-en protocol (see Figure 17). The inversion of Sanraku-en protocol for test subject YS was performed to improve the hydration effect of Biofangotherapy.

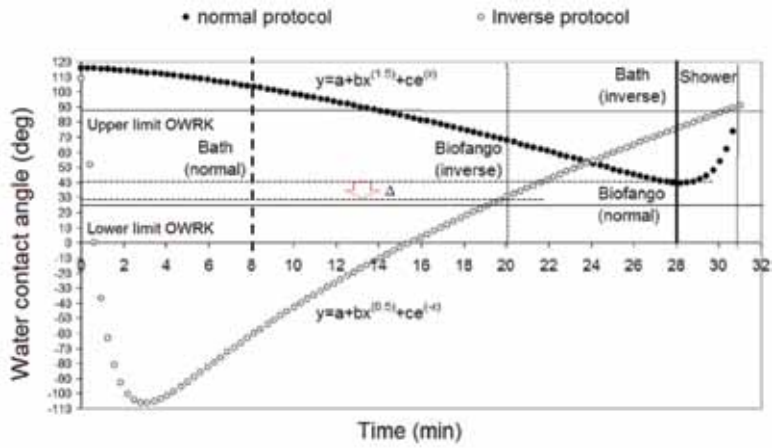

FIGURE 20
Comparison between normal and inverse dr-BPM diagrams of YS test subject. The red arrow indicates the increase of the hydration state of skin of YS test subject after the inversion of Sanraku-en protocol, however the water CA measured after the treatment remain over the lower limit of OWRK model (CA>24.8 deg).

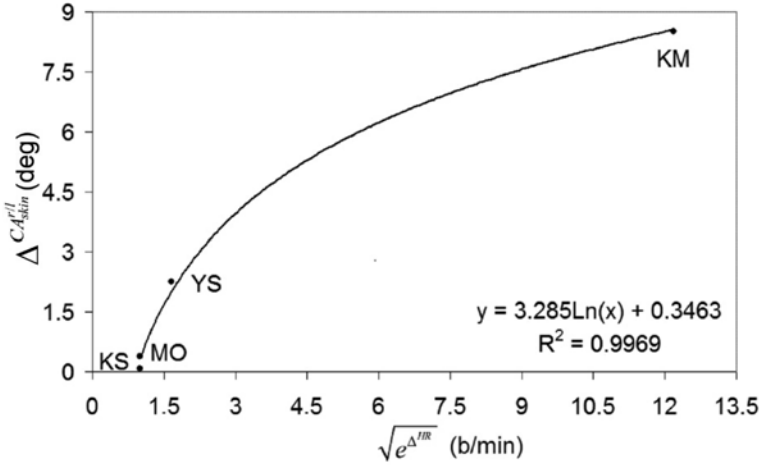

FIGURE 21
Correlation between the hydration state of skins of test subjects after BFM treatment (; deg) and heart rate parameters (; beats/min).

The positive result of the new procedure (see Figure 20) appeared to be in accordance with the "barrier effect" hypothesized based on the lowest variations of the surface energy parameters of BFM after the treatment (see Figure 17). The increase of the skin hydration of test subject YS led to the suggestion

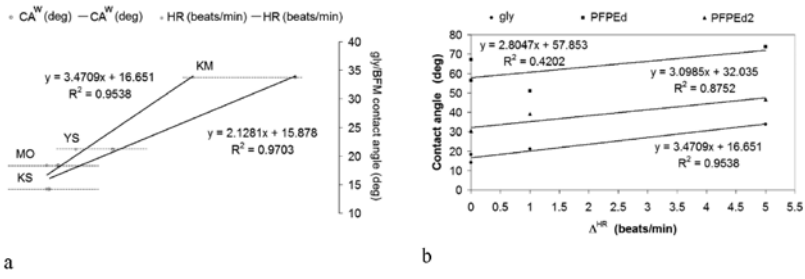

FIGURE 22
Correlation trends between (a) glycerol (gly) contact angles (deg) measured on exhaust (used) BFM and contact angles of water (CA^W; deg) measured on skin of test subjects after Sanraku-en mudtherapy protocol, and correlation between glycerol (gly) contact angles (deg) measured on exhaust (used) BFM and heart rate (HR; beats/min), and (b) correlation between contact angles (deg) of glycerol (gly), Fomblin HC/25® Perfluoropolyether (PFPEd), Fomblin HC/OH-1000® Perfluoropolyether (PFPEd2) measured on exhaust BFM and heart rate (D^{HR}).

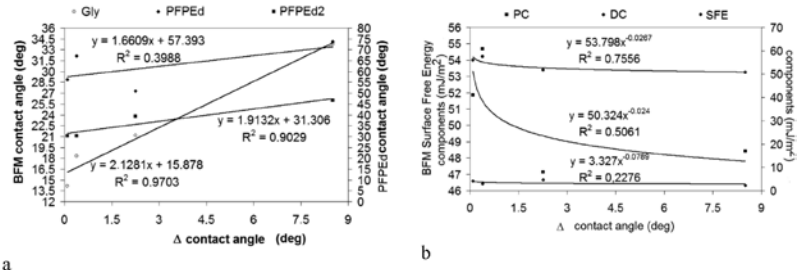

FIGURE 23
Correlations between (a) moisturize level of BFM (CA; deg) and hydration state of skin of test subjects after Sanraku-en mudtherapy protocol (D; deg) and between the same hydration state of skin of test subjects after Sanraku-en mudtherapy protocol (D; deg) and the CA (deg) of Fomblin HC/25® Perfluoropolyether (PFPEd) , and (b) correlation between the polar component (PC; mJ/m^2) of BFM and the hydration state of skin of test subjects after Sanraku-en mudtherapy protocol (D: deg).

that a plus time repetition of Biofango® treatment performed under control by dr-BPM method would be beneficial. In the case of test subject MO, the high hydration effect of BFM observed in Figures 13 (CA<24.8 deg) and 14, appeared to be correlated to the decrease of DC of the used mud and to the increase of CA of diiodomethane and Fomblin HC/25® Perfluoropolyether (PFPEd), which CAs were determined using the FCAM (TVS mud index). In this context, the FCAM demonstrated its great sensitivity in the CA measurements due to its low SFE (18.1 mN/m), DC (mN/m), PC (mN/m), and repulsion forces generated at the interface between Fomblin HC/25® Perfluoropolyether (PFPEd) and BFM. However, the used BFM characterized after the treatment of test subject KM showed an increase in TVS mud index values, stable levels

of PC, great loss of DC, and high CA of glycerol. This anomalous increase of CA of glycerol could be due to a possible loss of moisture from the skin surface of test subject KM (see Figure 15 and 19).

The development of dr-BPM diagram had allowed one to highlight the effect of physiological parameters such as heart rate on the hydration state of skin as a function of the forearms measurements area. In the end, the Figures 21, 22a, 22b, and 23a demonstrated clearly the link existing between physiological parameters and surface free energy and the possibility to easily measure them using surface tension technique.

6 CONCLUSIONS

The development of dr-BPM diagram allowed for the determination of a personalized way which changes the levels of hydration of the skin of each test subject. In addition, it has been shown that this can be analysed using a "single drop" of water as a test liquid for each Sanraku-en mudtherapy protocol, assessing the real moisturizing effects of Biofango® mud mixture (BFM) and evaluating the efficacy of the thermal protocol in use for each test subject in relation to the kind of mud applied. What is more, it has been shown that there is a correlation between them surface tensiometry and physiological data in order to demonstrate the influence of the physiologic parameters (D^{HR}) on skin ($\Delta^{CA^{r/l}_{skin}}$) in relation to the hydration state and the variations of the surface tensiometry parameters before and after treatment of exhaust BFM (CA^{BFM}_{gly}). The use of a MobilDrop DSA2 Tenskinmeter has allowed the development of a dr-BPM diagram for skin hydration evaluation while a static tensiometer DSA10 has been shown to be effective for determining the TVS mud index of BFM mud. Using Glycerol, Fomblin HC/25® Perfluoropolyether (PFPEd) and Fomblin HC/OH-1000® Perfluoropolyether (PFPEd2) as test liquids it was possible to develop a surface tensiometry model for Japanese Biofango® in order to evaluate the variations of surface free energy parameters of skin and BFM after Biofangotherapy and showed the correlation between BFM (CA^{BFM}_{gly}) and skin ($\Delta^{CA^{r/l}_{skin}}$) CA parameters. The correlation studies suggest the possible formation of a stable liquid phase between skin and BFM as means for an exchange activity at the interface. However, the data obtained in this research stage has low statistical significance due to the involvement of such a small number of test subject, although it can be considered a good base for the evaluation and applicability of these methodologies on a larger scale. The possible application of the dr-BPM method on a larger number of test subjects would confirm its validity as a fast "single drop" diagnostic tool capable to optimize and qualify the Sanraku-en/Biofango® protocol currently in use, depending on the moisturizing effects of different mixtures of Biofango® used. The implementation of a new triad of biocompatible liquid tests such as Fomblin HC/25® Perfluoropolyether (PFPEd)/Fomblin HC/OH-1000® Perfluoropolyether (PFPEd2)/Glicerol

98% could give rise to the optimization of surface free energy characterization of other geomaterials. Based on the correlations identified between functional and therapeutic effects of thermal mud and considering the actual Japanese people's viewpoint of mud therapy, the validation of these methods could be strategic for other spas, helping the diffusion of Biofango® and its mixtures as a preferred geomaterial for therapeutic use also.

7 AKNOWLEDGMENTS

The Author would like to thank Prof. Antonio Bettero (Senior Professor of University of Padova) that made possible the japanese mission in 2010, Mr Hikonari Sakai (Head of Sanraku-en Co.), and Miss Keiko (Sanraku-en Co.) for the mudpack treatment protocol, The Author would also like to acknowledge Prof. Kenji Sugimori (University of Toho), MrsYuko Sakai (Sanraku-en Co.), Mrs Mizuno Owada (Ascendant Co.) for their suggestions and support and Mr. Kazuhiro Matsuura (Marukoshi Co.) for the preparation of Biofango® mixtures.

This work is dedicated to the rememberance of the Tsunami disaster that shocked Japan on 11th March 2011, this research is fully dedicated to the Japanese people and the great courage demonstrated during the crisis and in these 8 years of reconstruction. The Author wants to express his admirable closeness to all the victims and their families with great friendship.

REFERENCES

[1] Khodambashi R., Najarian S. Golpaygani A.T., Keshtgar A. and Torabi S., A tactile sensor for detection of skin surface morphology and its application in telemedicine systems. *American Journal of Applied Sciences* **5** (2008) 633-638.

[2] Bloemen M.C.T., van Gerven M.S., van der Wal M.B.A., Verhaegen P.D.H.M. and Middelkoop E., An objective device for measuring surface roughness of skin and scars. *Journal of American Academic Dermatology* **64** (2011) 706-715.

[3] Leeson D.T., Meyers C.L. and Subramanyan K., In vivo confocal fluorescence imaging of skin surface cellular morphology: a pilot study of its potential as a clinical tool in skin research. *International Journal of Cosmetic Science* **28** (2006) 9–20.

[4] Darlenski R., Sassning S., Tsankov N. and Fluhr J. W., Non-invasive in vivo methods for investigation of the skin barrier physical properties. *European Journal of Pharmaceutics and Biopharmaceutics* **72** (2009) 295–303.

[5] Hendriks C. P. and Franklin S.E., Influence of Surface Roughness, Material and Climate Conditions on the Friction of Human Skin. *Tribology Letters* **37** (2009) 361–373.

[6] Wenzel R.N., Resistance of solid surfaces to wetting by water. *Industrial and Engineering Chemistry* **28** (1936) 988-994.

[7] Schott H., Contact angles and wettability of human skin. *Journal of Pharmacology* **60** (1971) 1893–1895.

[8] König B.E., Schäfer T., Huss-Marp J., Darsow U., Möhrenschlager M., Herbert O., Abeck D., Krämer U., Behrendt H. and Ring, J., Skin surface pH, stratum corneum hydration, trans-epidermal water loss and skin roughness related to atopic eczema and skin dryness

in a population of primary school children: Clinical report. *Acta Derm Venereol* **80** (2000) 188-191.

[9] Mavon A., Zahouani H., Redoules D. Agache P., Gall Y. and Humbert P., Sebum and stratum corneum lipids increase human skin surface free energy as determined from contact angle measurements: A study on two anatomical sites. *Colloids Surfaces B: Biointerfaces* **8** (1997) 147–155.

[10] Elkhyat A., Courderot-Masuyer C., Mac-Mary S., Courau S., Gharbi T. and Humbert P., Assessment of spray application of Saint GERVAIS® water effects on skin wettability by contact angle measurement comparison with bidistilled water. *Skin Research and Technology* **10** (2004) 283–286.

[11] Bettero A., Dal Bosco C., Gregorio M. and Veller Fornasa C., In vivo bioadhesivity evaluation by TVS skin test*,* International Proceedings of 13th EADV Congress. November 17-21 2004, Florence, Italy.

[12] Jobstraibizer P.G., Definizione mineralogica e chimica del fango termale Eugeneo*, Mineralogica et Petrographica Acta* **52** (1999) 317-37.

[13] Bettero A., Marcazzan M., Semenzato A., The quality of clays used for healing purposes. *Mineralogica et Petrographica Acta* **42** (1999) 277-286.

[14] Rossi D., Dobrzynski D., Moro I., Zancato M. and Realdon, N., The importance of an integrated analytic approach to the study of physic chemical characteristics of natural thermal waters used for pelotherapy aims: Perspectives for reusing cooled thermal waters for treatments related to thermalism applications. In: *Geothermal Water Management,* Bundschuh J. and Tomaszewska B. (Eds), Taylor&Francis Group, London, UK, **6** (2017) 365-389.

[15] Bader S., Brunetta F. and Pantini G., Perfluoropolyethers a new class of products for cosmetic applications. *International Proceedings of XIC I.F.S.C.C. Congress*. September 16-19 1986, Barcelona, Spain.

[16] Tonelli C., Gavezotti P. and Strepparola E., Linear perfuoropolyether difunctional oligomers: chemistry, properties and applications. *Journal of Fluorine Chemistry* **51** (1999) 90-95.

[17] Rossi D., Dal Bosco C., Jobstraibizer P.G., Setti M. and Bettero A., Thermal muds evaluation by Tensiometric Versus Skin modeling (TVS modeling), *International Proceedings of the I*st *Congresso Ibero Americano de Peloides.* November 5-7 (2007), Vigo, Espana.

[18] Rossi D. and Bettero A., Introduction to "TVS mud index" as an evaluation marker of silt-clayey matrices for bioadhesive thermal and cosmetic applications. *The Journal of The Japanese Society of Balneology, Climatology and Physical Medicine* **77** (2014) 457-458.

[19] Veniale F., Bettero A., Jobstraibizer P.G. and Setti M., Thermal muds: Perspectives of innovations. *Applied Clay Science* **36** (2007) 141-147.

[20] Rossi D., Rossi S., Morin H. and Bettero A., Within-tree variations in the surface free energy of wood assessed by contact angle analysis. *Wood Science & Technology* **46** (2012) 287-298.

[21] Rossi D., Mioni E., Zancato M., Bettero A. and Rossi S., Development of a tensiometric model for surface energy characterization of raw coffee beans. *Journal of Food Engineering* 112 (2012) 352–357.

[22] Sugimori K., Okajima M., Oowada M., Shankar S., Biofango®, modified for original style from Italian Fango, a method to use hot spring water for health promotion, *5th International Conference on Natural Products for Health and Beauty*, May 6–8 (2014), Thailand.

[23] Sugimori K., Oowada M., Microbiological studies for developments of Biofango® in Japan, *Italian Fango Congress*, November (2009), Abano Terme, Italy.

[24] Sugimori K., Microorganisms living in the extreme environments, hot springs and acidic conditions, *International seminar for Applied Biology on Fango Therapy and Heating Circulation*, May (2008), University of Padova, Padova, Italy.

[25] Sugimori K., Okajima M., Oowada M., The Utility of fangotherapy and the importance of adsorption of material onto the peloid, *All-Russian Scientific Conference with Foreign Participation*, September (2015), Vladivostok, Russia.

[26] Watanabe S., Italia Fangotherapy. The Japanese Society of Balneology, *Climatology and Physical Medicine* **75** (2011) 65-57.

[27] Aeimbhu A., Scanning electron microscope for characterising of micro and nanostructured titanium surfaces. *Scanning Electron Microscopy* **29** (2012) 578-588.

[28] Bortolozzi J.P., Banús E.D., Milt V.G., Gutierrez L.B. and Ulla M.A., The significance of passivation treatments on AISI 314 foam pieces to be used as substrates for catalytic applications. *Applied Surface Science* **257** (2010) 495–502.

[29] Leena K., Athira K.K., Bhuvaneswari S., Suraj, S. and Lakshmana Rao V., Effect of surface pre-treatment on surface characteristics and adhesive bond strength of aluminum alloy. *International Journal of Adhesion & Adhesives* **70** (2016) 265–270.

[30] Fowkes M.F., Attractive forces at interface. *Industrial and Engineering Chemistry* **56** (1964) 40-52.

[31] Owens D.K. and Wendt R.C., Estimation of the surface free energy of polymers. *Journal of Applied Polymer Science* **13** (1969) 1741- 1747.

[32] Zenkiewicz M., Methods for the calculations of surface free energy of solids. *Journal of Achievements in Materials and Manufacturing Engineering* **24** (2007) 137-145.

[33] Rabel W., Einige Aspekte der Benetzungstheorie und ihre Anwendung auf die Untersuchung und Veränderung der Oberflächeneigenschaften von Polymeren, *Farbe und Lack* **77** (1971) 997-1005.